Available online at www.sciencedirect.com
SCIENCE DIRECT®
ELSEVIER
Geoderma 112 (2003) 217–233
GEODERMA
www.elsevier.com/locate/geoderma

Kriging soil texture under different types of nonstationarity

M. Meul*, M. Van Meirvenne

Department of Soil Management and Soil Care, Ghent University, Coupure 653, 9000 Gent, Belgium

Received 16 November 2001; accepted 14 October 2002

Abstract

A geostatistical analysis assumes some form of stationarity of the variable under study, but different types of stationarity exist and often spatial data exhibit some form of nonstationarity. However, most studies assume one type of nonstationarity and consequently apply one type of interpolation method within the study area.

A study area of 8 × 18-km area was selected because it was expected to contain complex nonstationary conditions in soil texture. Therefore, four geostatistical interpolation methods were evaluated in their ability to account for different types of nonstationarity in the topsoil silt content: two univariate interpolation methods, ordinary kriging (OK) and universal kriging (UK), and two bivariate methods, simple kriging with varying local means (SKlm) and ordinary cokriging (OCK). A digital elevation model (DEM) was used as the exhaustive secondary information for the bivariate methods.

Two kinds of nonstationary conditions were identified inside the study area: (1) a large-scale trend in both the silt content and elevation, with a strong correlation between them, and (2) a very strong local fluctuation around a mean value, representing a local nonstationarity. Consequently, different techniques were applied in different parts inside the study area: the global trend was best accounted for by OCK and UK could best account for the local nonstationarity. After combining the results of the two prediction methods, it was found that the overall estimation of the silt content was more precise than when any single method was used over the entire study area.

Keywords: Kriging; Nonstationarity; Spatial trend; Soil texture

* Corresponding author.
E-mail address: marijke.meul@rug.ac.be (M. Meul).

PII: S0016-7061(02)00308-7

1. Introduction

Geostatistical interpolation methods are frequently used to describe the spatial variation of natural phenomena. In their basic form, these interpolation methods assume some form of stationarity of the variable under study, in order to comply with the underlying theory of Random Functions (Journel and Huijbregts, 1978; Armstrong, 1998). Depending on the definition, different types of stationarity can be assumed: strict stationarity, second-order or weak stationarity, intrinsic stationarity or quasi-stationarity (Journel and Huijbregts, 1978).

Another aspect of stationarity is its scale-dependence. A phenomenon may appear stationary locally, whereas it may be nonstationary over longer distances, e.g. in the presence of a large-scale trend. Or the opposite may occur: under general stationary conditions, strong local fluctuations may appear, indicating a local nonstationarity.

Thus, stationarity is not an unambiguous concept and the presence of stationarity depends on the circumstances that we work under. Moreover, the assumptions of stationarity are often violated in practice; Cressie (1986) argued that data virtually never exhibit stationarity. Also, the presence of spatial trends in soil parameters and soil catenas evolving from physical factors are common (Gotway Crawford and Hergert, 1997). According to Webster (2000), we should ask ourselves the question whether the assumption of a stationary model of the soil is reasonable in these circumstances and whether it is profitable in that it can lead to accurate predictions.

In geostatistics, there are several ways to incorporate trends and account for nonstationarity; and several authors have described and compared some of these techniques (Cressie, 1986; Journel and Rossi, 1989; Gotway Crawford and Hergert, 1997). However, in most of those studies, only one type of nonstationarity is considered and one single interpolation technique is applied for the whole study area.

The purpose of this study was (1) to examine how we can account for different types of nonstationarity present inside one study area and (2) to explore which method to use under various conditions. Therefore, we selected a study area of 8×18 km, which was expected to exhibit complex nonstationarity conditions in the topsoil silt content. We applied four geostatistical interpolation methods under two different assumptions: in the first case, only one type of nonstationarity was considered and the methods were used uniformly over the whole study area; in the second case, different types of nonstationarity were assumed inside the study area and multiple interpolation methods were applied at different locations after which the results were combined. The four interpolation methods included two univariate methods, ordinary kriging (OK) and universal kriging (UK), and two bivariate methods, ordinary cokriging (OCK) and simple kriging with varying local means (SKlm).

An independent test set was used to evaluate the prediction performances of the different interpolation methods and to evaluate which method, or combination of methods, performed best.

2. Theory and methods

The following gives a brief review of the applied kriging methods. More detailed presentations are given in geostatistical handbooks (e.g. Journel and Huijbregts, 1978; Goovaerts, 1997; Wackernagel, 1998).

Geostatistics is based on the concept of Random Functions (RF), whereby the set of attribute values $z(\mathbf{x})$ at all locations $\mathbf{x}$ are considered as a particular realization of a set of spatially dependent Random Variables (RV) $Z(\mathbf{x})$. To make this approach acceptable, certain assumptions have to be made, which are introduced under the hypothesis of stationarity.

2.1. The hypothesis of stationarity

In the strictest sense, a RF is stationary when all the moments of its distribution are invariant under translation (Armstrong, 1998).

In geostatistics, often only the first two moments of the RF are considered, called *second-order* or *weak stationarity*. A RF is said to be weakly stationary when the mathematical expectation $\mathrm{E}[Z(\mathbf{x})]$ exists and does not depend on the support point $\mathbf{x}$:

$$\mathrm{E}[Z(\mathbf{x})] = m \quad \forall \mathbf{x} \tag{1}$$

and when for each pair of RV $\{Z(\mathbf{x}), Z(\mathbf{x}+\mathbf{h})\}$, the autocovariance exists and depends on the separation distance $\mathbf{h}$:

$$C(\mathbf{h}) = \mathrm{E}[Z(\mathbf{x}+\mathbf{h}).\ Z(\mathbf{x})] - m^2 \quad \forall \mathbf{x}. \tag{2}$$

This hypothesis can be reduced when assuming stationarity of the first two moments of the increments of the RF, termed *intrinsic stationarity*. This assumes that the mean and variance of the increments $\{Z(\mathbf{x}+\mathbf{h}) - Z(\mathbf{x})\}$ exist and are independent of $\mathbf{x}$:

$$\mathrm{E}[Z(\mathbf{x}+\mathbf{h}) - Z(\mathbf{x})] = 0 \quad \forall \mathbf{x}$$

$$\mathrm{Var}[Z(\mathbf{x}+\mathbf{h}) - Z(\mathbf{x})] = \mathrm{E}[\{Z(\mathbf{x}+\mathbf{h}) - Z(\mathbf{x})\}^2] = 2\gamma(\mathbf{h}) \quad \forall \mathbf{x} \tag{3}$$

where $\gamma(\mathbf{h})$ is the semivariance.

In practice, the semivariance is only used for distances $|\mathbf{h}| \le b$, where b represents the radius of a circular neighbourhood of estimation. The limitation of the hypothesis of second-order or intrinsic stationarity to those bounded distances corresponds to the hypothesis of *quasi-stationarity*.

These different definitions of stationarity automatically lead to different definitions of nonstationarity. Nonstationary conditions are present:

1. when the mathematical expectation of the RV (Eq. (1)) is not independent of the support point $\mathbf{x}$, in other words, when the local mean value changes with location,
2. when the semivariance (Eq. (3)), or the covariance (Eq. (2)), does not only depend on the separation distance, but changes with direction or location.

Nonstationarity is also scale-dependent. A global nonstationarity can be caused by a large-scale trend, or a local nonstationarity may be present when the variable seems stationary over a longer distance, but shows strong fluctuations on a local scale.

2.2. Ordinary kriging

Ordinary kriging (OK) is one of the most basic kriging methods. At an unsampled location $\mathbf{x}_0$, Z is estimated by:

$$Z^*(\mathbf{x}_0) = \sum_{i=1}^{n} \lambda_i Z(\mathbf{x}_i)$$

where $Z^*(\mathbf{x}_0)$ is the estimated value of the RV Z at the unsampled location $\mathbf{x}_0$ and λ_i are the n weights assigned to the observation points $Z(\mathbf{x}_i)$. The weights λ_i sum to one to assure unbiased conditions and they are found by minimizing the estimation variance.

The RV $Z(\mathbf{x})$ can be decomposed into a trend component $m(\mathbf{x})$ and a residual component $R(\mathbf{x})$:

$$Z(\mathbf{x}) = m(\mathbf{x}) + R(\mathbf{x}). \tag{4}$$

OK assumes stationarity of the mean and considers $m(\mathbf{x})$ to be a constant, but unknown, value. Nonstationary conditions are taken into account by restricting the domain of stationarity to a local neighbourhood and moving it across the study area. The residual component $R(\mathbf{x})$ is modeled as a stationary RV with zero mean and under the assumption of intrinsic stationarity, its spatial dependence is given by the semivariance $\gamma_R(\mathbf{h})$:

$$\gamma_R(\mathbf{h}) = \frac{1}{2}\mathrm{E}[\{R(\mathbf{x}+\mathbf{h}) - R(\mathbf{x})\}^2]. \tag{5}$$

Assuming a constant mean $m(\mathbf{x})$, Eq. (5) is equivalent to:

$$\gamma(\mathbf{h}) = \frac{1}{2}\mathrm{E}[\{Z(\mathbf{x}+\mathbf{h}) - Z(\mathbf{x})\}^2].$$

2.3. Universal kriging

Universal kriging (UK) considers that $m(\mathbf{x})$ (Eq. (4)) is not constant, but that it varies smoothly within the local neighbourhood, representing a local trend. The trend $m(\mathbf{x})$ is recalculated within each local neighbourhood. This trend component is modeled as a weighted sum of known functions $f_l(\mathbf{x})$ and unknown coefficients a_l, $l = 0,\ldots L$ (Journel and Rossi, 1989):

$$m(\mathbf{x}) = \sum_{l=0}^{L} a_l f_l(\mathbf{x}).$$

Often low order polynomials of the coordinates **x** are used to express the trend model.

In practice, the residual semivariance $\gamma_R(\mathbf{h})$ (Eq. (5)) is calculated before the trend $m(\mathbf{x})$ is modeled. Since the attribute values $z(\mathbf{x})$ are the only available data, the residual semivariance is calculated by selecting pairs of observations that are not or slightly affected by the trend.

2.4. Simple kriging with varying local means

In Simple kriging with varying local means (SKlm), the unknown local stationary mean $m(\mathbf{x})$ of the OK estimate is replaced by known varying local means $m^*(\mathbf{x})$ derived from secondary information which must be known at any location $\mathbf{x}_0$. The linear estimator is written as:

$$Z^*(\mathbf{x}_0) = m^*(\mathbf{x}_0) + \sum_{i=l}^{n} \lambda_i R(\mathbf{x}_i)$$

where $m^*(\mathbf{x}_0)$ is the estimated mean for the location $\mathbf{x}_0$ and $R(\mathbf{x}_i)$ are the residuals of the n observation points: $R(\mathbf{x}_i) = Z(\mathbf{x}_i) - m^*(\mathbf{x}_i)$.

The local means can be derived from the secondary information using a relation of the type:

$$m^*(\mathbf{x}_0) = f[y(\mathbf{x}_0)] = a_0 + a_1\, y(\mathbf{x}_0)$$

where a_0 and a_1 are the regression coefficients and $y(\mathbf{x}_0)$ is the value of the secondary variable Y at location $\mathbf{x}_0$.

The residual component $R(\mathbf{x})$ is modeled as a stationary RV with zero mean and a spatial dependence is given by the semivariance $\gamma_R(\mathbf{h})$ (Eq. (5)).

Goovaerts (1999) found that SKlm gave similar results as kriging with an external drift. Therefore, the latter was not considered here.

2.5. Ordinary cokriging

Ordinary cokriging (OCK) is a multivariate extension of OK, in which the estimator is calculated by using simultaneously the auto-correlation between the primary data and the spatial cross-correlation between primary and secondary variables (Myers, 1982).

In this case study, standardized cokriging was used. In this method, the secondary variable is rescaled, so that its mean equals that of the primary variable. The cokriging estimator is then written as:

$$Z^*(\mathbf{x}_0) = \sum_{i=1}^{n1} \lambda_i Z(\mathbf{x}_{1i}) + \sum_{j=1}^{n2} \rho_j [Y(\mathbf{x}_{2j}) - m_Y + m_Z]$$

where m_Z and m_Y are the means and λ_i and ρ_j are the weights of the primary and secondary variable, respectively.

Unbiased conditions are assured by the following condition:

$$\sum_{i=1}^{n1} \lambda_i + \sum_{i=1}^{n2} \rho_i = 1$$

and the weights λ_i and ρ_j are found by minimizing the estimation variance.

3. Study area and data set

As a study area, a rectangular area of 8 × 18 km, located in the province of East-Flanders, Belgium (Fig. 1) was selected. This particular area was chosen because we expected the presence of a general form of nonstationarity in soil texture, based on our prior knowledge and information on the pedological and topographical properties of the region. In a more general study, Van Meirvenne (1991) proposed a stratification of East-Flanders into six major soil texture regions, three of which are located inside this study area (Fig. 2a):

(i) a sand to loamy sand region in the northern part, dominated by texture classes Z, S and P according to the Belgian texture triangle (Tavernier and Maréchal, 1962);
(ii) a sandy loam to silt loam transition area in the central part, represented mainly by texture class L;
(iii) a silt loam to silt region in the southern part, containing mainly texture class A.

A digital elevation model (DEM) (Fig. 2b) shows that the topography is also nonstationary: elevation ranges between 10 m in the N and 95 m in the S.

Soil texture data were available from the Belgian soil survey at 189 locations. Additionally 71 soil samples were taken and analyzed, which resulted in a total data set

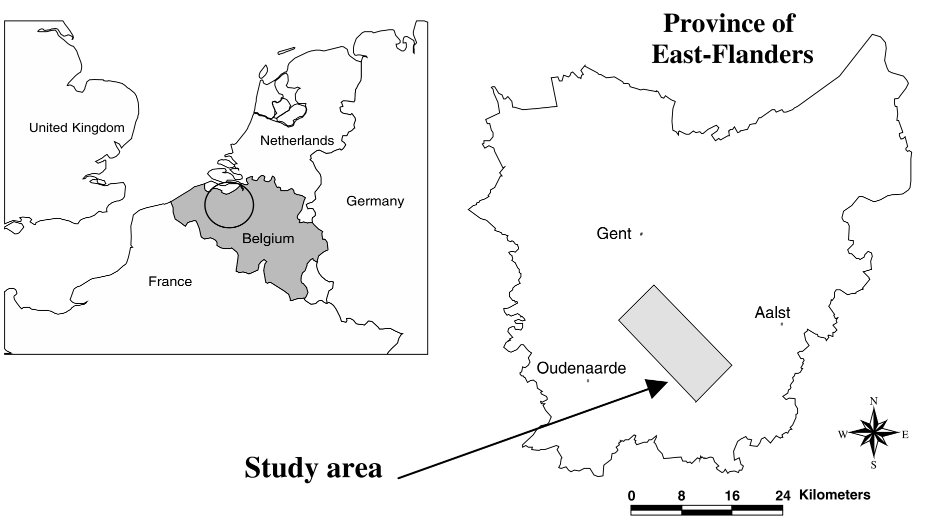

Fig. 1. Location of the study area within Belgium and the province of East-Flanders.

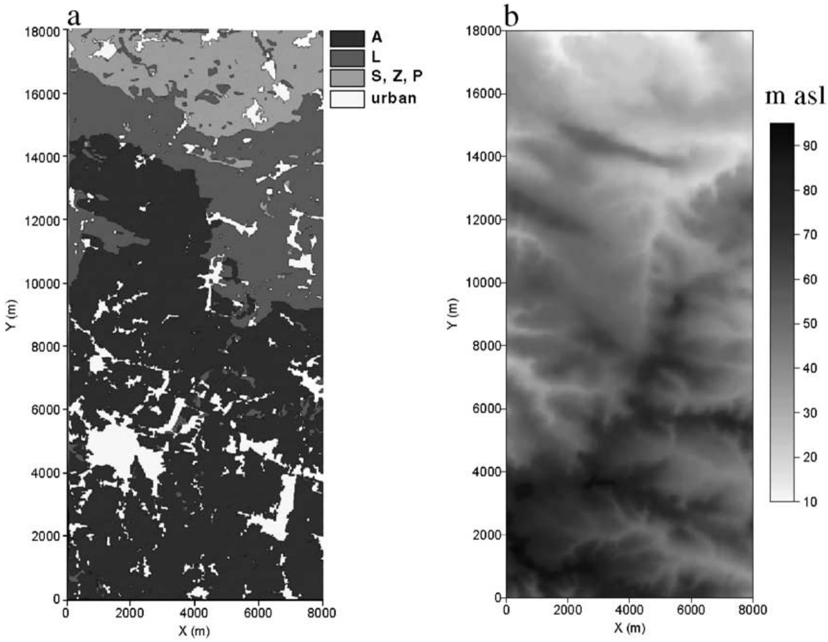

Fig. 2. The available information of the study area: (a) the different soil texture classes taken from the Belgian soil map (legend: see text) and (b) a digital elevation model.

of 260 texture samples. We used the silt fraction as a target variable because this fraction changed most within the area. A histogram and summary statistics of the silt content are shown in Fig. 3a. Fig. 3b shows a location map of the silt content at the 260 observation points. The data clearly reflect the global pattern of soil texture shown in Fig. 2a. However, the point data indicate that there are considerable fluctuations in the silt content inside the silt region, which are not revealed by the texture classes of the soil map.

To validate the performance of the different methods, we randomly split up the total data set into 96 work data, which were used for the application of the interpolation methods, and 164 validation points, which constituted an independent test set.

4. Results and evaluation of the interpolation methods

4.1. Assuming a uniform type of nonstationarity

The interpolation methods were applied uniformly over the whole study area, assuming that one type of nonstationarity was present. The topsoil silt content was predicted using OK, UK, OCK and SKlm. Each method was hereby applied twice:

(i) The work data set was used to estimate silt at the 164 points of the validation set, allowing to evaluate the performance of the different methods.
(ii) The total data set of 260 points was used to map the silt fraction.

Fig. 4 shows the experimental variograms and the fitted models of the four interpolation methods, based on the 96 observations of the work data set.

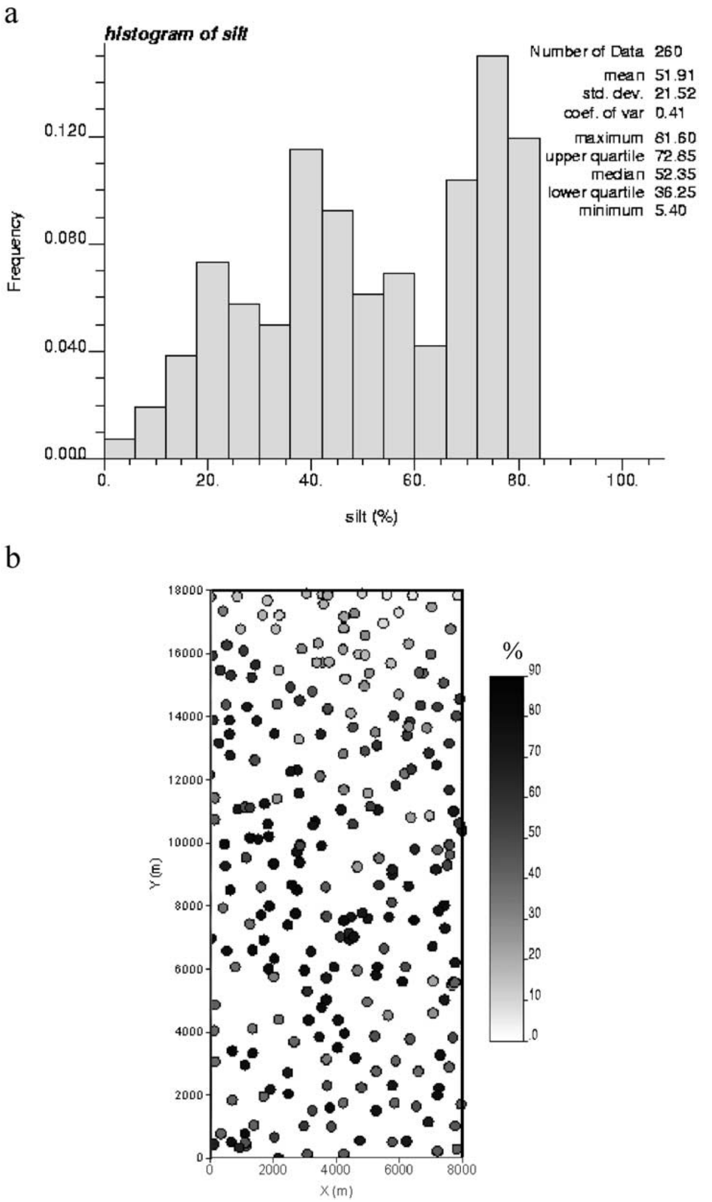

Fig. 3. (a) Histogram and summary statistics of the silt content and (b) silt content at 260 observation points.

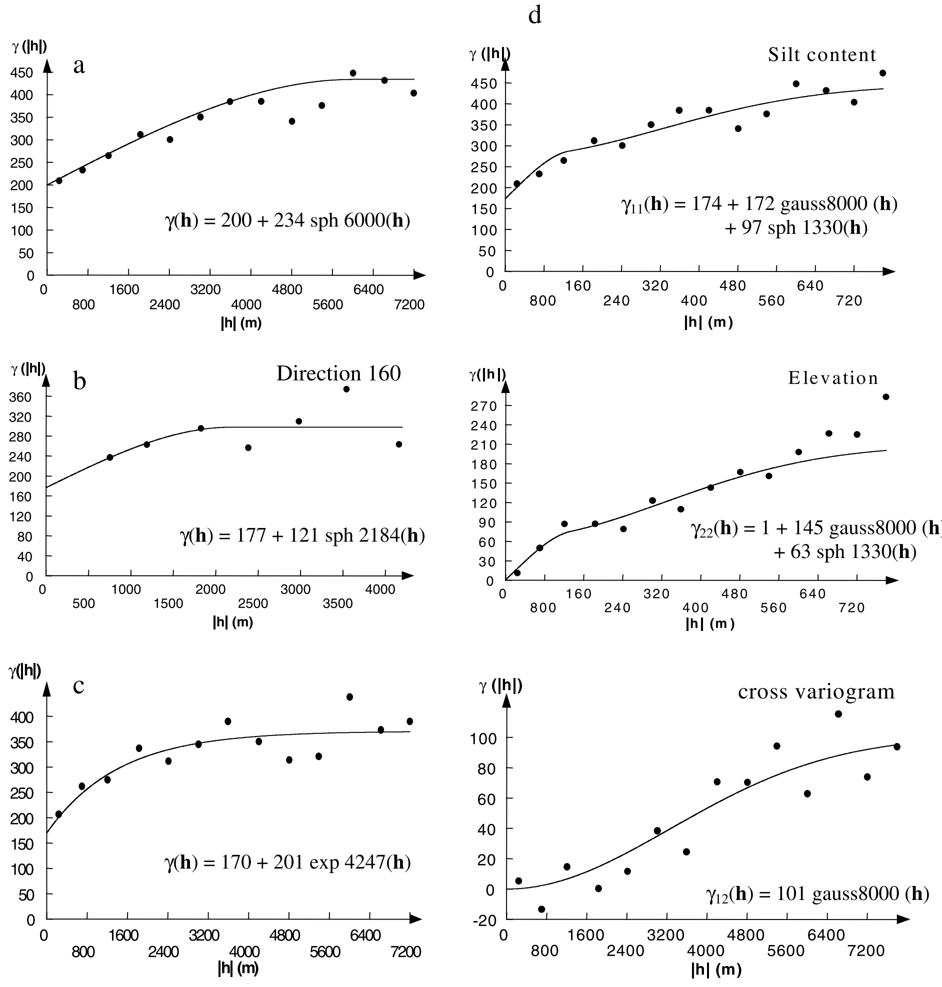

Fig. 4. (a) Experimental variogram and fitted model used in OK, (b) directional experimental variogram and fitted model used in UK, (c) residual variogram and fitted model used in SKlm and (d) experimental variograms of primary and secondary variables and cross-variogram and fitted models used in OCK.

For the bivariate interpolation methods, the DEM (Fig. 2b) was used as an exhaustive secondary information source, since elevation was known at every estimation point. Fig. 5 shows the positive correlation between the silt content and elevation. However, the correlation coefficient was rather weak (0.47).

The interpolation methods were compared by re-estimating the data values of the independent test set using observations of the nonoverlapping work data set, after which the true and estimated values were compared (Efron, 1982; Voltz and Webster, 1990).

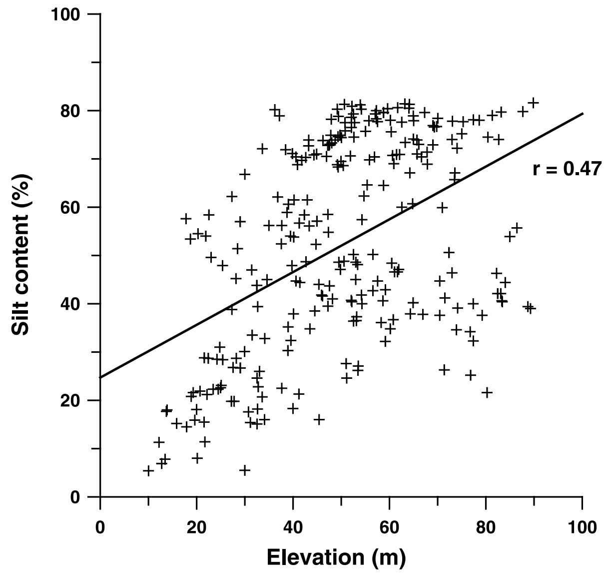

Fig. 5. Scattergram between primary variable (silt content) and secondary variable (elevation) and the linear model fitted with a correlation coefficient of 0.47.

The Mean Squared Estimation Error (MSEE), which calculates the averaged squared difference between the true value $Z(\mathbf{x})$ and the estimated value $Z^*(\mathbf{x})$, was used as an evaluation index:

$$\mathrm{MSEE} = \frac{1}{m}\sum_{i=1}^{m}[Z^*(\mathbf{x}_i) - Z(\mathbf{x}_i)]^2$$

with m the number of observation points in the independent test data set (here $m = 164$). Obviously, the value of MSEE should be as small as possible.

OK, which assumes local stationarity, was considered as a reference method to assess the ability of the other methods to account for the nonstationary conditions. The validation results are given in Table 1. Two limits for the MSEE could be taken into account when interpreting these results. An upper limit could be obtained by using the global mean of the

Table 1
Mean Squared Estimation Error of the silt content of the four interpolation methods for the whole study area

Interpolation methods	MSEE ($\%^2$)
Global average	480
OK	259
UK	250
OCK	258
SKlm	298

work data as a prediction for every point of the test data set. This resulted in an MSEE of 480%^{2}. The nugget effect of the omnidirectional variogram model could be considered as a lower limit, since it gives an average indication of the noise present inside the study area. This nugget effect was 200%^{2} (Fig. 4a). It can be observed that all interpolation methods performed much better than the global mean, but the best method (UK) resulted in a MSEE of 250%^{2}.

The results show furthermore that the MSEE of OK, UK, and OCK did not significantly differ from each other: OCK produced a similar MSEE as OK and UK was slightly better. SKlm performed much worse. Surprisingly, the best estimation of the topsoil silt content was obtained by a univariate method and no actual gain was taken from incorporating the elevation values into the estimation of the silt content. Yet, based on geological history, elevation and texture were expected to be closely related, since the soils inside the study area developed in eolian sediments. Apparently, the correlation with the secondary variable was too weak to gain from using bivariate methods. Under such circumstances of weak correlation, SKlm performs even worse than the univariate methods and therefore its use is not recommended in such case.

The need to account for the nonstationarity in soil texture however was indicated by the best performance of UK.

Fig. 6 shows the interpolated maps of silt content obtained by the different interpolation methods, using the entire data set. UK, OK and OCK, which show little difference in MSEE, also show similar maps, with the same global pattern but some differences at a more detailed scale. SKlm, which had a much higher MSEE, shows a map that is quite different from the other interpolations, due to the strong influence of the secondary variable.

4.2. Assuming different types of nonstationarity

Next, we assumed that different types of nonstationarity were present inside the study area. This assumption was based on Fig. 7, which shows the fluctuations of silt content and elevation along the longitudinal axis of the study area.

In this figure, the general behavior of the elevation is shown by considering this variable along a transect at $X = 4000$ m (Fig. 2b). The silt content was calculated as the average per Y-intervals of 500 m for X going from 0 to 8000 m (Fig. 3b). Based on Fig. 7, we concluded that the relationship between both variables behaves differently within the study area: (1) for $Y < 7000$ m (southern part) both variables show a more or less stationary mean, but with strong local fluctuations around it; (2) for $Y > 7000$ m (northern part), a clear spatial trend can be observed for both variables. So, inside the study area, we encountered two types of nonstationarity: local nonstationarity in the S part and a global nonstationarity in the N part.

We considered the delineation between the two parts (set at $Y = 7000$ m) as a gradual transition separating two strata with different structures of spatial variation. In this method, described by Boucneau et al. (1998), the delineation is considered as a stratification of the interpolation methods, but not of the observations involved in the interpolation.

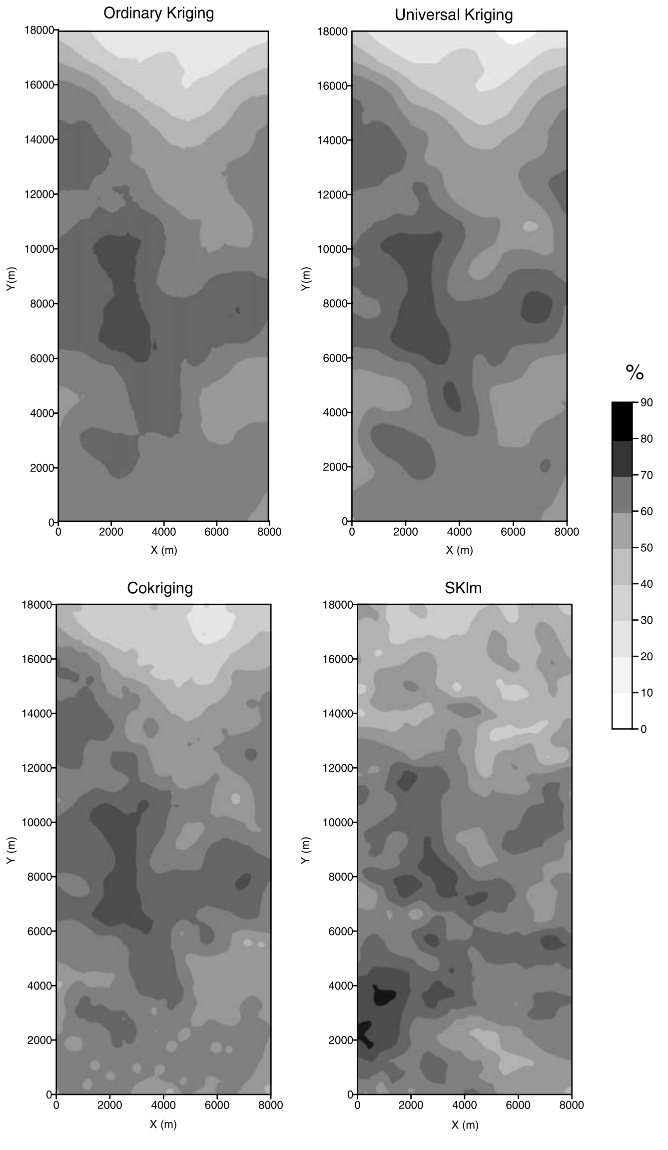

Fig. 6. Interpolated maps of the topsoil silt content.

4.2.1. The N part (large-scale trend)

The N part shows a large-scale trend in both the silt content and elevation and these variables show a rather strong correlation ($r = 0.69$), as can be seen from Fig. 7 (subset, top right).

Within this part, we disposed of 172 observation points of silt. The work data set now consisted of 67 observations (including a number of locations situated in the S part to

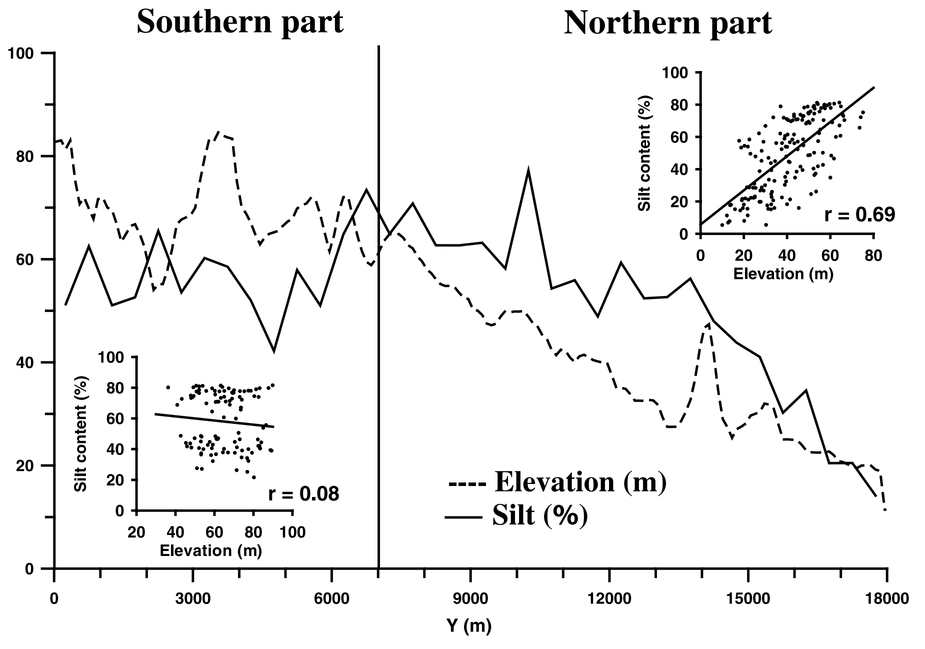

Fig. 7. Elevation along a transect located at $X = 4000$ m and silt content per step of $Y = 500$ m. In subset: scattergrams between silt and elevation for both parts (< or > than $Y = 7000$ m).

ensure continuity across the delineation of both sub parts of the study area) and the validation data set contained 105 observations. The experimental variograms and fitted models of the four interpolation methods are shown in Fig. 8. The values of the test data points were estimated by the four interpolation methods and the validation was done as before.

The results are shown in Table 2. As expected, the bivariate interpolation methods now resulted in the lowest MSEE, where OCK gave better results than SKlm. This can be explained by the fact that SKlm only uses the secondary information to calculate the moving average, while OCK explicitly uses the values of the secondary variable in the estimation of the primary variable. The univariate methods UK and OK performed similar. Despite the fact that there is a clear trend inside the area, the ‘nonstationary’ interpolation method UK did not give a better estimation than the ‘stationary’ estimator OK did. So, using OK with a moving window allows to incorporate a global trend, assuming local stationarity.

4.2.2. The S part (local nonstationarity)

At first sight, second-order stationary conditions can be assumed in this part of the study area, but the presence of strong local fluctuations may cause a local nonstationarity. Fig. 7 (subset, left bottom) shows that the correlation between elevation and silt is insignificant ($r = 0.08$) due to the irregular topography. Application of the bivariate methods was clearly useless, hence only OK and UK were applied.

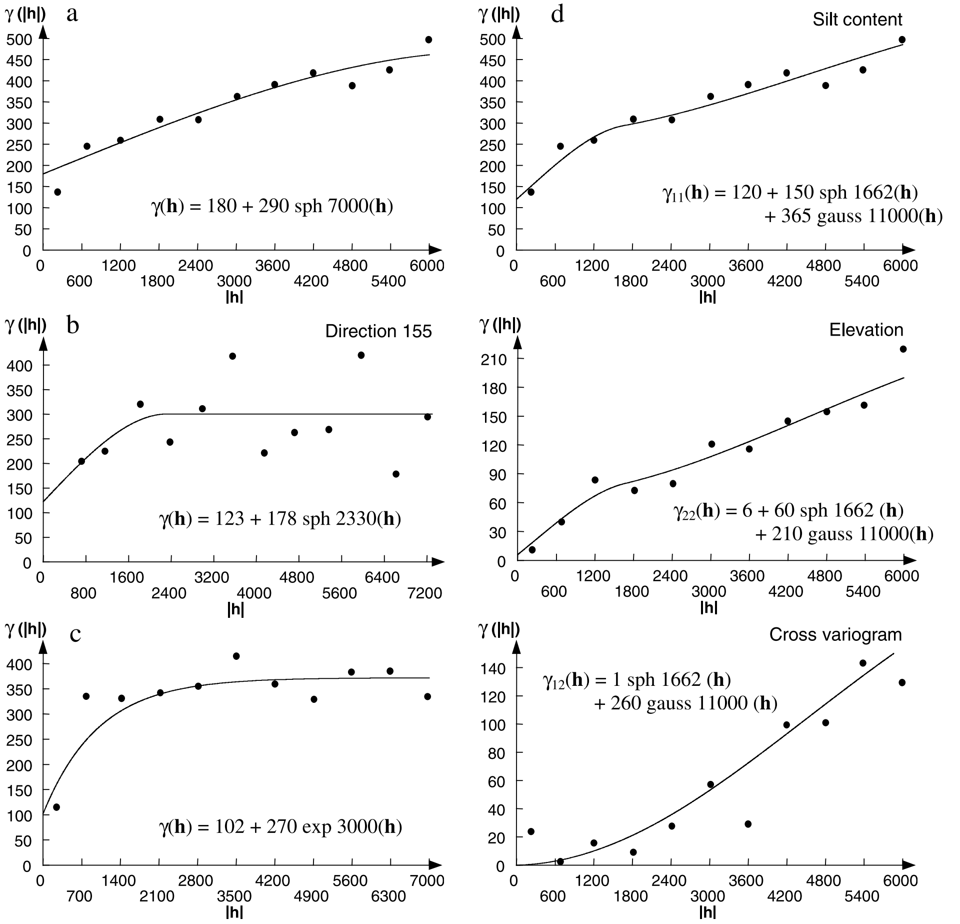

Fig. 8. Variograms and models used in the interpolation of the northern part of the study area: (a) experimental variogram and fitted model used in OK, (b) directional experimental variogram and fitted model used in UK, (c) residual variogram and fitted model used in SKlm and (d) experimental variograms of primary and secondary variables and cross-variogram and fitted models used in OCK.

The available data set consisted of 107 observation points, with a work data set of 48 points (again with some overlap with the N part to ensure continuity across the dividing line) and a test data set of 59 locations. The experimental variograms and fitted models for OK and UK are shown in Fig. 9.

The results of the validation of the methods can be found in Table 2. UK resulted in the lowest MSEE, despite the apparent stationary conditions. Strong local fluctuations cause local nonstationary conditions, which were better accounted for by UK. OK has been found to be very sensitive to short-range variation before (Laslett and McBratney, 1990), and our findings confirm this. The MSEE of both interpolation methods were higher when compared to the values found for the N part

Table 2
Mean Squared Estimation Error of the silt content of the interpolation methods after separation into two parts (N and S) and their combination (entire study area)

Interpolation methods		MSEE (%^{2})
N (*Y*>7000 m)	OK	223
	UK	226
	OCK	197
	SKlm	219
S (*Y*<7000 m)	OK	309
	UK	298
Entire study area	UK + OCK	234

of the study area, which indicates larger estimation errors for the silt content within this part.

4.2.3. Combining the N and S parts

The MSEE of the entire study area was calculated by comparing the true values of the 164 validation points with their estimations, using OCK in the N part and UK in

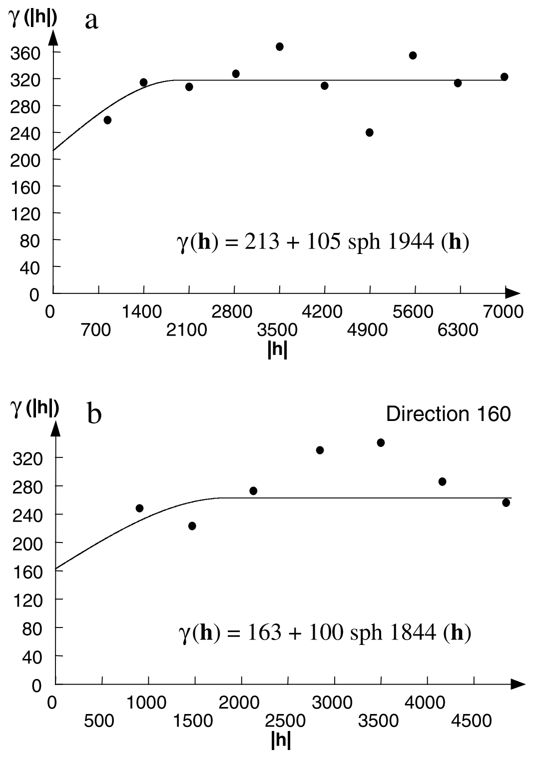

Fig. 9. Variograms and models used in the interpolation of the southern part of the study area: (a) experimental variogram and fitted model used in OK, (b) directional experimental variogram and fitted model used in UK.

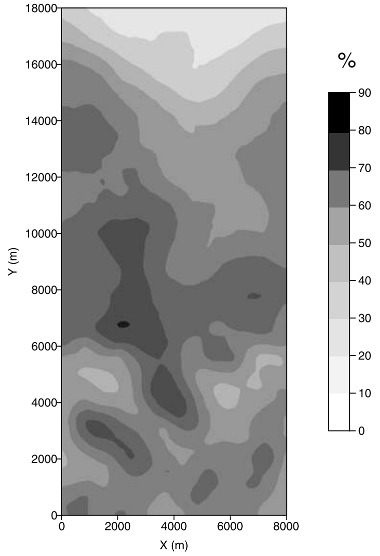

Fig. 10. Map of the silt content for the total study area after merging the two parts, using cokriging in the northern part (Y>7000 m) and UK in the southern part (Y< 7000 m).

the S part. This resulted in a MSEE of 234%^{2} (Table 2), which is considerably lower than the smallest value of the MSEE obtained by using a single method for the whole study area (250%^{2}, Table 1).

A map of silt of the whole study area was obtained by merging the interpolations of both parts using the best performing method for each part: OCK in the N part and UK in the S part (Fig. 10). This map clearly reflects the presence of a global trend in silt in the N part of the study area (Y>7000 m), followed by local nonstationary conditions causing strong local fluctuations in silt content in the S part (Y< 7000 m).

5. Conclusions

We evaluated four geostatistical interpolation methods in their ability to account for different nonstationary conditions in soil texture. When considering one type of nonstationarity for the whole study area, OCK could not improve the estimation relative to the univariate UK, which performed the best, despite the availability of an exhaustively sampled secondary variable. It was found that in the situation where there is a weak correlation (r less than 0.5) between the primary and secondary variable, SKlm even performs worse than the univariate OK.

This survey showed that different interpolation methods gave the best results under different forms of nonstationarity. In the N part of the study area, there was a large-scale trend which represented a global nonstationarity. In this area, a good correlation between elevation and silt content was present ($r = 0.69$). This resulted in better interpolation results obtained with the bivariate interpolation methods, with OCK performing the best. The ‘stationary’ method OK could account for this global trend even slightly better than the ‘nonstationary’ UK, because it allows to use a local neighbourhood and to assume quasi-stationarity.

In the S part of the study area, a more complex, local nonstationarity in soil texture was present, caused by strong fluctuations around a mean value. Here UK gave the best estimation of the silt content.

After combining the interpolations of both parts, the estimation of the silt content improved considerably, compared to using any of the applied methods uniformly over the whole study area.

Therefore, we recommend that in situations where a nonstationary behavior is expected, it is closely investigated whether there are more types of nonstationarity present. Identifying these types of nonstationarity allows choosing the appropriate interpolation method for each type, rather than applying a single method over the entire study area.

References

Armstrong, M., 1998. Basic Linear Geostatistics. Springer, New York.

Boucneau, G., Van Meirvenne, M., Thas, O., Hofman, G., 1998. Integrating properties of soil map delineations into ordinary kriging. Eur. J. Soil Sci. 49, 213–229.

Cressie, N., 1986. Kriging nonstationary data. J. Am. Stat. Assoc. 81, 625–634.

Efron, B., 1982. The Jackknife, The Bootstrap, and Other Resampling Plans. Soc. for Industrial and Applied Math., Philadelphia.

Goovaerts, P., 1997. Geostatistics for Natural Resources Evaluation. Oxford Univ. Press, New York.

Goovaerts, P., 1999. Using elevation to aid the geostatistical mapping of rainfall erosivity. Catena 34, 227–242.

Gotway Crawford, C.A., Hergert, G.W., 1997. Division S-8—Nutrient management and soil and plant analysis. Incorporating spatial trends and anisotropy in geostatistical mapping of soil properties. Soil Sci. Soc. Am. J. 61, 298–309.

Journel, A.G., Huijbregts, C.J., 1978. Mining Geostatistics. Academic Press, London.

Journel, A.G., Rossi, M.E., 1989. When do we need a trend model in kriging? Math. Geol. 21, 715–738.

Laslett, G.M., McBratney, A.B., 1990. Further comparison of spatial methods for predicting soil pH. Soil Sci. Soc. Am. J. 54, 1553–1558.

Myers, D.E., 1982. Matrix formulation of cokriging. Math. Geol. 14, 249–257.

Tavernier, R., Maréchal, R., 1962. Soil survey and soil classification in Belgium. Transactions of a Joint Meeting of the International Soil Science Society, New Zealand, 13–22 November. Wright and Carman Ltd., Wellington, pp. 298–307.

Van Meirvenne, M., 1991. Characterization of soil spatial variation using geostatistics. PhD thesis, Ghent University, Belgium.

Voltz, M., Webster, R., 1990. A comparison of kriging, cubic splines and classification for predicting soil properties from sample information. J. Soil Sci. 41, 473–490.

Wackernagel, H., 1998. Multivariate Geostatistics. Springer, Berlin.

Webster, R., 2000. Is soil variation random? Geoderma 97, 149–163.